J. Chem. Thermodynamics 101 (2016) 64–77

Contents lists available at ScienceDirect

J. Chem. Thermodynamics

journal homepage: www.elsevier.com/locate/jct

Liquid glycerol: Experimental densities at pressures of up to 25 MPa, and some derived thermodynamic properties

Nieves M.C.T. Prieto [a], Thiago A. Souza [b], Ana P. Egas [a], Abel G.M. Ferreira [a,*], Lélio Q. Lobo [a], António T.A. Portugal [a]

[a] Departamento de Engenharia Química, Faculdade de Ciências e Tecnologia, Universidade de Coimbra, Pólo II, Rua Sílvio Lima, 3030-790 Coimbra, Portugal
[b] Universidade Federal Rural do Rio de Janeiro, Brazil

ARTICLE INFO

Article history:
Received 7 February 2016
Received in revised form 13 May 2016
Accepted 14 May 2016
Available online 17 May 2016

Keywords:
Glycerol
Density
Equation of state
Vapour pressure
Enthalpy of vapourisation

ABSTRACT

In spite of the importance of glycerol in industry, only limited consistent information on its *pVT* data seems to be available in the literature. In this work, the density of glycerol (1,2,3-propanetriol) was measured within the temperature range 298.15–348.15 K and over the pressure range from atmospheric pressure up to 25.0 MPa by means of a vibrating tube densimeter. The estimated combined standard uncertainty of measurements is 0.86 kg·m^{-3}. The experimental *pVT* values of this study combined with selected values from the literature covering the ranges of T = (278–373) K and of p = (0.1–200) MPa were fitted using the Goharshadi–Morsali–Abbaspour equation of state (GMA EoS). The measured density in this work correlates with deviations of ±0.05% (less than 0.5 kg·m^{-3}) and in the range ±0.1% with the overall results. From the GMA EoS, the mechanical coefficients as thermal expansivity, isothermal compressibility and internal pressure were calculated. Vapour pressures selected from the literature covering the temperature range between the triple point and the normal boiling point were correlated with the Wagner equation. This equation was used in conjunction with the Clapeyron equation to calculate the molar enthalpies of vapourisation from the triple point to the normal boiling point.

1. Introduction

The density of liquid glycerol (1,2,3-propanetriol) has been measured since the early years of the eighties in the nineteenth century but the experiments carried out by Bridgman [1] were the first ones covering extensive temperature ranges and made up to high pressures. In spite of the importance of glycerol both on theoretical and practical grounds, only a few consistent studies on density have been published since that pioneering work. Moreover, much of the information available for the density of the liquid at atmospheric pressure is fragmentary and derives from studies on binary mixtures [2]. This led us to make measurements of this property from 298.15 K to 348.15 K and pressures of up to 25 MPa using a vibrating tube densimeter. The existing data in the literature were also assessed and those considered the most reliable were combined with our own measurements and treated by using the equation of state due to Goharshadi–Morsali–Abbas pour (GMA EoS) [3]. This equation of state has been found to be adequate for polar, non-polar, and H-bonded fluids. Some of the mechanical coefficients of the liquid such as the thermal expansivity, the isothermal compressibility, and the internal pressure were calculated from the equation of state and compared with values from the literature.

In addition to the density of the liquid, the development of chemical processes involving glycerol often requires the knowledge of accurate vapour pressure data and of the enthalpy of vapourisation. Due to the very strong molecular association in the liquid phase, glycerol has a lower vapour pressure than would be expected from its molar mass. Accurate values of vapour pressure for glycerol are scarce and those existent lie in the micron range (<10^{-3} torr), usually measured by effusion techniques, are inconsistent. The values for vapour pressures higher than 1 kPa have often been obtained from ebulliometry or using static apparatus. In this work, reliable vapour pressures selected from the literature, including the critical point coordinates measured by Nikitin et al. [4], were correlated by using the well-known Wagner equation [5]. The values of the enthalpy of vapourisation were also evaluated from the triple point temperature to the normal boiling temperature.

* Corresponding author.
E-mail address: abel@eq.uc.pt (A.G.M. Ferreira).

http://dx.doi.org/10.1016/j.jct.2016.05.006
0021-9614/

2. Experimental

2.1. Chemicals

Glycerol was obtained from Sigma–Aldrich (CAS number 56-81-5) with stated mass fraction purity (GC) $\geqslant$0.995 (water by Karl Fisher $\leqslant$0.001). Since glycerol is highly hygroscopic, samples were degassed ultrasonically, dried over freshly activated molecular sieves (Type 3 Å) supplied by Aldrich and further purified by evaporation in a rotary evaporator working at 343 K. The water content was determined with a Metrohm 831 Karl Fisher coulometer indicating that the purification procedure reduced the water mass fraction from 1.3×10^{-3} to 7×10^{-4}.

2.2. Density measurements

Liquid densities were measured using an Anton Paar DMA 60 digital vibrating tube densimeter with a DMA 512P measuring cell, within the temperature range from 298.15 K to 348.15 K and over pressures from 0.10 MPa to 25.0 MPa. The measuring setup and the calibration of the vibrating tube densimeter were described in detail in a previous paper [6]. The temperature in the vibrating tube cell was measured with a platinum resistance probe with standard uncertainty $u(T) = 0.01$ K. The probe was previously calibrated over the range 273.15–373.15 K against a platinum resistance thermometer ERTCO-Eutechnics High Precision Digital Thermometer certified in the ITS90. A Julabo F12-ED thermostatic bath with ethylene glycol as circulating fluid was used in the thermostat circuit of the measuring cell held constant to ±0.01 K. The required pressure was generated and controlled with a Pressure Generator model 50-6-15, High Pressure Equipment Co., using acetone as hydraulic fluid. The diameter of the metallic tube used in the measurements was 1.59 mm, the buffer being longer than 1 m to guarantee the inexistence of back diffusion of the hydraulic liquid into the liquid contained in the densimeter cell. Pressures were measured with a pressure transducer (Wika Transmitter S-10, WIKA Alexander Wiegand GmbH & Co.) with a maximum standard uncertainty of $u(p) = 0.03$ MPa. An NI PCI-6220 data acquisition board (DAQ) from National Instruments (NI) was used for the real time registration period, temperature, and pressure values. For this task, a Labview application was developed. Modules of temperature (NI SCC-FT01) and pressure (NI SCC-CI20) were installed in a NI SC-2345 carrier and connected to a DAQ board. Taking into account four values of the period of oscillation at every (T,p) state the precision of the density measurements is of the order of ±0.1 kg·m^{-3}.

The influence of viscosity on the density uncertainty (due to damping effects on the vibrating tube) can be of some importance in liquid glycerol because of the high values of that property in the range of the density measurements. For liquids with viscosities less than 100 mPa·s this uncertainty can be obtained by using an equation given by the Anton Paar suppliers [7] for the DMA512P densimeter.

$$\Delta\rho/\rho = (-0.5 + 0.45\sqrt{\eta}) \cdot 10^{-4} \quad (1)$$

where ρ represents the density value obtained from the DMA512P densimeter, $\Delta\rho$ is the difference between this density value and the corrected density due to the effect of the viscosity of the liquid, and η is the dynamic viscosity (in mPa·s). For viscosities higher than 400 mPa·s, the viscosity correction factor becomes constant and equal to 0.5 kg·m^{-3} [8]. Between (100 and 400) mPa·s, the viscosity correction shows intermediate behaviour. From the measured densities in this work and the viscosities at atmospheric pressure measured by Shankar and Kumar [9] and Cook et al. [10] over the overall temperature range from 273.15 K to 398.15 K, the uncertainty in density due to viscosity is about 0.5 kg·m^{-3} at temperatures lower than 308.15 K, and 0.3 kg·m^{-3} for higher temperatures. The combined standard uncertainty of the density measurements, estimated taking into account the influence of uncertainties associated with calibration equation [6], temperature, pressure, period of oscillations (six-digit frequency counter), viscosity, and density data of calibrating fluids was $u_c(\rho) = 0.86$ kg·m^{-3}. The expanded uncertainty with confidence level 95% (coverage factor $k = 2$) was estimated to be $U(\rho) = 1.7$ kg m^{-3}.

3. Results and discussion

3.1. Fixed points and sources of data

For the normal melting temperature of glycerol, Wilhoit et al. [11] selected the value $T_m = (291.8 \pm 0.2)$ K reported by Volmer and Marder [12] who made the measurements by carefully protecting a dry sample from atmospheric moisture. This value has been given as the triple point temperature T_p by NIST [13] and was considered as such in the present work. The only measurements of the critical temperature T_c and critical pressure p_c have been made by Nikitin et al. [4] who used the method of pulse heating a wire probe placed in the liquid obtaining $T_c = 850$ K and $p_c = 7500$ kPa. For unstable decomposing liquids as glycerol, they found that the critical temperature depends on the heating time. The extrapolation of duration of heating for zero gives $T_c = 850$ K. The critical temperature and pressure presented by Nikitin et al. [4] were selected for this work and they can be compared with the values $T_c = 726$ K, and $p_c = 6680$ kPa tabulated by Reid et al. [14]. These authors have selected $T_b = 563.15$ K as the temperature at the normal boiling point and this value is usually used in reference works.

The density studies over wide ranges of temperature and pressure can be summarized as follows. Bridgman [1] used a variable-volume cell with bellows and used the density of liquids at 273.15 K as reference to obtain fractional changes of volume. McDuffie et al. [15] developed a variable-volume cell with bellows and the densities of pressurized liquid were found from measured values at atmospheric pressure. This author did not provide the measured values of density giving instead the graphical representation of data with Tait equation of state. Khelladi et al. [16] used a vibrating U-tube densimeter to make the density measurement of density as function of temperature at atmospheric pressure. They used these values and the experimental measurements of speed of sound in the range 283–373 K and pressures up to 100 MPa combined with the heat capacity at atmospheric pressure to calculate the density at those ranges of temperature and pressure applying an iterative technique. Khelladi et al. [16] compared their calculated density results with the values from Tait EoS reported by Cibulka et al. [17] and deviations lower than 0.2% (less than 3 kg·m^{-3}) were found. Some few indirect determinations of density as a function of pressure come from experimental compressions made by Nakagawa et al. [18], by Miyamoto et al. [19] and by Egorov and Makarov [20]. Walsh and Rice [21] and Dick [22] reported densities at very high pressures. Extensive data at atmospheric pressure (determinations in temperature ranges of 50 K length or more) come from Adamenko [23], Khelladi et al. [16], Egorov and Makarov [24] and Egorov et al. [2].

The density values for glycerol measured in this work are reported in Table 1 and plotted in Fig. 1 as a function of pressure and temperature. All the experimental values show that density has the expected behaviour with the temperature and pressure: the increase with pressure for isothermal conditions and the drop of density as temperature increases at fixed pressure. Another conclusion is that the purification process of glycerol had no influence

Table 1
Experimental values of density of glycerol ρ as a function of temperature T and pressure p.

ρ/(kg·m^{-3}) at T/K								
p/MPa	298.15	303.15	308.15	313.15	318.15	328.15	338.15	348.15
Purified liquid[a]								
0.1	1258.4	1255.7	1252.9	1250.1				
5.0	1260.7	1257.8	1254.9	1251.8				
10.0	1262.3	1259.3	1256.3	1253.4				
15.0	1263.7	1260.8	1257.9	1254.9				
20.0	1265.2	1262.3	1259.4	1256.4				
25.0	1266.6	1263.7	1260.8	1257.9				
Supplied liquid [b]								
0.1	1259.1		1253.0		1247.0	1240.9	1234.8	1228.7
5.0	1260.6		1254.6		1248.5	1242.5	1236.4	1230.4
10.0	1262.1		1256.1		1250.1	1244.1	1238.1	1232.1
15.0	1263.6		1257.6		1251.6	1245.6	1239.6	1233.6
20.0	1265.1		1259.1		1253.2	1247.2	1241.3	1235.3
25.0	1266.5		1260.6		1254.7	1248.8	1242.9	1237.1

Standard uncertainties u are as follows: $u(T) = 0.01$ K, $u(p) = 0.03$ MPa, $u_c(\rho) = 0.86$ kg·m^{-3}.
[a] After degassed ultrasonically, dried over freshly activated molecular sieves and further purified in a rotary evapourator.
[b] As supplied by Sigma–Aldrich (with stated mass fraction purity (GC) ⩾0.995).

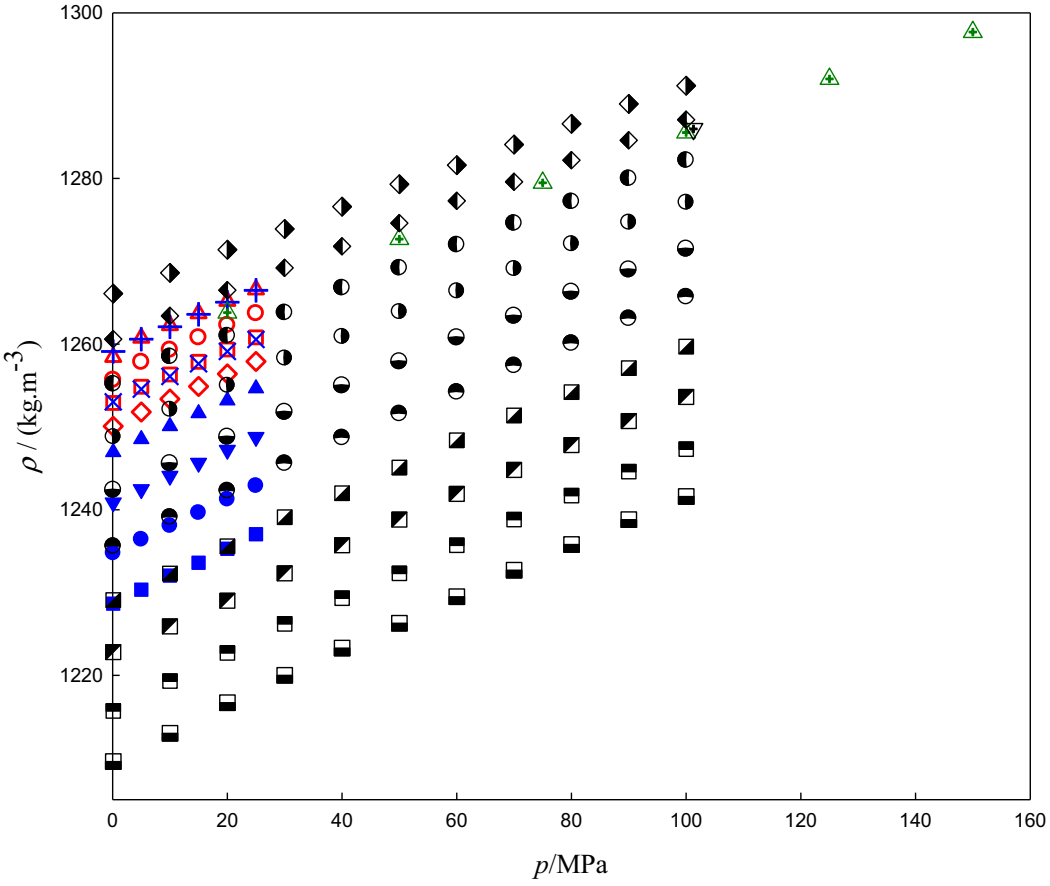

Fig. 1. Isotherms of the density of glycerol as function of the pressure. Legend: This work purified (p) and non-purified (np) glycerol: △, 298.15 K (p); +, 298.15 (np); ○, 303.15 K (p); □, 308.15 K (p); ×, 308.15 (np); ◊, 313.15 K (p); ▲, 318.15 (np); ▼, 328.15 K (np); ●, 338.15 K (np); ■, 348.15 K (np); ▽, 298.15 [18]; ⟁, 298.15 K [19]; ◭, 283.15 [16]; ◮, 293.15 K [16]; ◐, 303.15 K [16]; ◑, 313.15 K [16]; ◒, 323.15 K [16]; ◓, 333.15 K [16]; ◪, 343.15 K [16]; ◩, 353.15 K [16]; ⬒, 363.15 K [16]; ⬓, 373.15 K [16].

on density: the two sets of data do not differ by more than 0.3 kg·m^{-3}. Our values at 298.15 K are in good agreement with those from Miyamoto et al. [19]. The density by these authors at pressures higher than 25 MPa follows the trend defined by our experimental values. By comparing our results with others from the literature at overlapping pressures and temperatures, we conclude that densities by Khelladi et al. [16] are in close agreement with our values: at temperatures 303.15 K and 313.15 K and pressures p = (0.1, 10, 20) MPa, the deviations between the two sets of data are less than 0.1% (less than 1.3 kg·m^{-3}). Comparing with data from Egorov et al. [20] at T = (298, 308) K and p = (0.1, 10, 25 MPa) the maximum deviation is 1.6 kg·m^{-3} at 308.15 K and 10 MPa. Taking the literature values available at 0.1 MPa the maximum deviation is 2.0 kg·m^{-3} at 338.15 K for data reported by Ge et al. [25] and

Table 2
Sources of data for the density of glycerol.

Authors	Year	N_p	ΔT/K	ΔP/MPa	$(\Delta\rho)(u_\rho)$ [a]	Method[b]	Purity/mass fraction
Bosart and Snoody [35]	1928	4	288.15–298.15	0.1	(1262–1265) (not stated-ns)	PYC	(ns)
P.W. Bridgman [1]	1932	43	273.15–368.15	49–1177	(1206–1432) (ns)	VB	ns
Walsh and Rice [21]	1957	2	291.15,303.15	7660,17030	(1256,1263)	SW	DIST
Darbari et al. [36]	1967	3	313.15–333.15	0.1	(1234–1247) (ns)	PYC	ns
McDuffie et al. [15][c]	1969	90	223–353	0.1–274.6	(1220–1365) (0.05%)	VB[c]	($3{\cdot}10^{-3}$ water)
Dick [22]	1981	13	295	860–56100	(1384–2471) (1.7%)	SW	0.995
Nakagawa et al. [18][d]	1983	1	298.15	101.3	1285.98 (0.2%)	MP	ns
Miyamoto et al. [19][d]	1990	8	298.15	20–200	(1264–1309) (0.3)	MP	>0.99
Xu et al. [37]	2003	2	298.15,308.15	0.1	(1254,1244) (0.01)	VTD	0.995
Adamenko et al. [23]	2006	13	290.35–355.95	0.1	(1224–1267) (ns)	PYC	DIST
Li et al. [38]	2007	8	298.15–333.15	0.1	(1236–1259) (0.3)	PYC	>0.999
Alkindi et al. [39]	2008	1	294	0.1	(1262) (ns)	VTD	0.998
Romero et al. [40]	2008	6	283.15–308.15	0.1	(1253–1266) (0.05)	PYC	0.99
Khelladi et al. [16]	2009	110	283–373	0.1–100	(1209–1291) (0.05%)	VTD	ns
Ge et al. [25]	2010	9	298.15–338.15	0.1	(1233–1258) (1%)	PYC	>0.997
Egorov and Makarov [24]	2012	6	293.15–348.15	0.1	(1226–1261) (0.05)	VTD	0.995
Palani and Srinivasan [26]	2012	3	303–313	0.1	(1251–1258)	PYC	ns
Kijevcanin et al. [41]	2013	3	293–303	0.1	(1255–1261) (0.3)	VTD	0.995
Koohyar et al. [42]	2013	3	303–323	0.1	(1243–1256)	VTD	0.98
Egorov et al. [2]	2013	8	278.15–348.15	0.1	(1226–1271) (0.05)	VTD	>0.995
Egorov and Makarov [20]	2014	30	278.15–323.15	0.1–100	(1242–1299) (0.05)	VTD and CVP	>0.995 ($2{\cdot}10^{-4}$ water)

[a] The uncertainty in density (u_ρ) is given in kg·m^{-3} or percentage. Upper and lower limits of density were rounded to integer values.
[b] SW: Shock wave; VB: variable-volume cell with bellows; MP: Mercury compression in Pyrex-glass piezometer; VTD: vibrating tube densimeter; PYC: pycnometer; CVP: constant volume piezometer.
[c] Following the author the calculated density from Tait EoS is accurate to better than 1 part in 2000.
[d] Density $\rho(T,p)$ was calculated from $\rho(T,p) = \rho_0(298.15\ \text{K}, p = 0.1\ \text{MPa})/(1-k)$ with experimental compression $k(T,p)$ and density $\rho_0(T,p) = 1258.4$ kg·m^{-3} measured in this work.

Table 3
Sources of data for the vapour pressure of glycerol.

Authors	Year	N_p	ΔT/K	$(\Delta p^\sigma)\ u(p^\sigma)$[a]	Method[b]	Purity/mass fraction
Richardson [30]	1886	53	391.6–533.6	(32–51400) (ns)	EBUL	DIST,VAC[c]
Kailan [43]	1912	15	443.7–466	(1600–4266) (ns)		0.998
McEwen [44]	1923	1	561.3	(95392) (ns)	EBUL	BIDIST
Mayer-Bugstrom [45]	1924	15	483.15–563.15	(5333–101325) (ns)		
Stedman [31]	1928	16	323.15–473.15	(0.33–6133) (27)	EBUL	0.998
Ziĺberman and Granovskaya [27][d]	1940	4	327–471	(0.67–6.7) (ns)	EFF	ns
Filosofo et al. [46]	1950	3	298–323	(0.027–0.29) (ns)	FM	ns
Ross and Heideger [28]	1962	17	296.9–340.2	(0.023–1.73) (0.13)	EFF	DIST
Cammenga et al. [29]	1977	16	291.13–341.35	(0.009–1.973) (ns)	EFF	DIST/DRY
Tang and MunkelWitz [47]	1991	11	297–328	(0.0012–0.419) (ns)	DE	0.995
Tatavarti et al. [48]	2002	6	443–448	(2266–2835) (ns)	TGA	0.99
Yan and Suppes [49]	2008	5	463–543	(3901–63429) (<91)	TGA	0.999
Soujanya et al. [32]	2010	8	497–561	(14190–95300) (ns)	EBUL	DIST
Mokbel et al. [33]	2012	11	351.8–462.86	(5.83–4099) (variable)	ST	0.99
Veneral et al. [34]	2013	5	477.3–520.7	(6700–33300) (ns)	EBUL	0.995

[a] The uncertainty in vapour pressure, $u(p)$, is given in Pa or percentage.
[b] EBUL: Ebuliometry; EFF: Effusion; FM: Fibre manometer; DE: Drop evaporation; TGA: Thermogravimetric; ST: Static.
[c] DIST,VAC: distilled in vacuum.
[d] Data given by E.E. Hughes, S.G. Lias, Vapour pressures of organic compounds in the range below one millimeter of mercury, NBS Technical Note 70, October 1960.

at 303.15 K for those by Palani and Srinivasan [26]. All the deviations are usually less than 0.15% meaning absolute deviations less than the expanded uncertainty of our measurements.

The vapour pressure of glycerol was measured by several techniques covering the whole range (291–561) K and (9×10^{-3}–95.392×10^3) Pa. The experimental techniques for determination of vapour pressures in the micron range are based on molecular effusion as the measurements made by Ziĺberman and Granovskaya [27], Ross and Heideger [28], Cammenga et al. [29]. In this range of vapour pressure, values show appreciable scattering and the error evaluation is difficult. The ebuliometric methods covered extensive ranges of vapour pressure and they were applied for the first time by Richardson [30] at the end of nineteen century, some years later by Stedman [31] and recently by Soujanya et al. [32], Mokbel et al. [33], and Veneral et al. [34]. The accuracy in the vapour pressure measurements from ebuliometric methods is difficult to evaluate and is only provided in the work by Stedman [31]. Mokbel et al. [33] used two static apparatuses for operation at different range of vapour pressures and with corresponding different uncertainties.

The information selected from the literature concerning the density and vapour pressure is presented in Tables 2 and 3, respectively. The characteristics of data such as the temperature and pressures ranges, numbers of experimental values, measurement method, and purity of samples are given whenever possible. The type of data is referred following the notation of Cibulka et al. [17] which work represents an important milestone with regard to critical review in the *pVT* state of art for glycerol.

3.2. Correlation of density

The GMA EoS was used to correlate the density at various temperatures and pressures. The GMA EoS is [3]:

$$(2z-1)V_m^3 = A(T) + B(T)\,\rho_m \tag{2}$$

where z, V_m, and ρ_m are the compressibility factor, molar volume, and molar density, respectively. Under isothermal conditions, the quantity $(2z-1)V_m^3$ as a function of molar density gives a straight line with intercept $A(T)$ and the slope $B(T)$. The temperature dependencies of the parameters $A(T)$ and $B(T)$ are given by the equations [3]:

$$A(T) = A_0 - \frac{2A_1}{RT} + \frac{2A_2 \ln T}{R} \quad (3)$$

$$B(T) = B_0 - \frac{2B_1}{RT} + \frac{2B_2 \ln T}{R} \quad (4)$$

where A_0–A_2 and B_0–B_2 are fitting parameters, and R is the gas constant.

The density values from this work were combined with selected values from the literature to form a working set to be used to obtain the parameters A_i and B_i by least squares fitting of Eq. (2). The selected values from the literature belong to two categories. In the first, values of density were included with the aim to establish the equation of state in pressure and temperature ranges where the existing experimental data have sufficient accuracy. The second category included the density values used to test the EoS. Within the first category, values at atmospheric pressure were used which correspond to sufficiently pure samples and (or) reduced uncertainty of data. In this same category, authors who reported density values as a function of pressure and temperature with either good purity of samples or low uncertainty of the measures were included. To test the EoS some existing literature values were used either at atmospheric pressure or at medium, high and very high pressure. In this test very recent studies were included. The values determined by Khelladi et al. [16], those derived from experimental compressions reported by Nakagawa et al. [18] and Miyamoto et al. [19] were included in the set and the values of Li et al. [38], Romero et al. [40], Ge et al. [25], Palani and Srinivasan [26], Kijevcanin et al. [41], Egorov et al. [2] measurements at atmospheric pressure were also included. The data reported by Egorov and Makarov [20] up to 100 MPa and those reported by Walsh and Rice [21] and Dick [22] at very high pressures (up to 56.1 GPa) were chosen to test the extrapolation performance of Eq. (2).

The coefficients A_0–A_2 and B_0–B_2, the standard deviation, σ, correlation coefficient, R^2, number of data points used in the fitting N_p and the standard deviation in density σ_ρ are given in Table 4. The working set provides a reliable equation of state to the calculation of density of glycerol for temperatures in the range 283.15–373.15 K and pressures up to 200 MPa with a standard deviation σ_ρ = ±0.8 kg·m^{-3} and average absolute deviation of AAD = ±0.05%.

Table 4
Parameters A_0–A_2, and B_0–B_2 of Eq. (2), temperature and pressure ranges (T_{min}, T_{max}, p_{min}, p_{max}), standard deviation σ, squared correlation coefficient r^2, number of data points N_p, and standard deviation on density σ_ρ.

M/(g mol^{-1})	92.094
A_0/(dm^9·mol^{-3})	3.360874 ± 0.637576
A_1/(MPa·dm^{12}·mol^{-2})	0.828606 ± 0.126983
A_2/(MPa·dm^{12}·mol^{-2})	−2.03909·10^{-3} ± 3.9062 · 10^{-4}
B_0/(dm^{12}·mol^{-4})	−0.252621 ± 4.68723 · 10^{-2}
B_1//(MPa·dm^{15}·mol^{-3})	−6.08292·10^{-2} ± 9.32235 · 10^{-3}
B_2/(MPa·dm^{15}·mol^{-3})	1.53954·10^{-4} ± 2.87242 · 10^{-5}
T_{min}/K	278.15
T_{max}/K	373.15
p_{min}/MPa	0.10
p_{max}/MPa	200.0
σ/(dm^9·mol^{-3})	5.584 · 10^{-5}
r^2	0.996
σ_ρ/(kg·m^{-3})	0.78
N_p	216
$AAD(\rho)$%	0.05

Fig. 2 shows $(2z-1)V_m^3$ as a function of molar density ρ_m in the range (283.15–373.15) K. The linearity holds between $(2z-1)V_m^3$ and ρ_m and the good consistency of density measured in this work with data by Miyamoto et al. [19] extending to 200 MPa is remarkable.

The density of the liquid at a given (T, p) state was calculated by solving Eq. (2) for ρ_m,

$$B(T)\,\rho_m^5 + A(T)\,\rho_m^4 + \rho_m - 2p/RT = 0 \quad (5)$$

The ability of GMA EoS to reproduce the density values at different temperatures and pressures was evaluated from the calculation of relative deviations. The comparison of the experimental values with the calculated values of density from Eq. (5) as a function of the temperature and pressure is made in Fig. 3. The GMA EoS correlates the experimental density of this work with deviations which are usually in the range ±0.1% (corresponding to deviations of less than ±1 kg·m^{-3}). The AAD% values obtained for the different sets of data are: this work 0.05%, Miyamoto et al. 0.03%, Kellady 0.05%, Nakagawa 0.02%, Egorov 0.09%, Palani 0.11%, Romero et al. 0.04%, Li et al. 0.04%, Ge et al. 0.08%, Kijevcanin et al. 0.07%. The data of Miyamoto et al. [19] deviate from GMA EoS by less than ±0.05% (less than ±0.7 kg·m^{-3}) up to 200 MPa.

Fig. 4 shows the relative deviations between density calculated from GMA EoS and the experimental values at atmospheric pressure for data included in the fitting with Eq. (2). Deviations are usually lower than 0.1% (less than 1 kg·m^{-3}). The relative deviations for excluded data are represented as a function of temperature in Fig. 5. The deviations from Bosart and Snoody [35] (given as reference in some studies) are progressively higher with increasing temperature reaching deviations of −0.3% at 298.15 K. The measurements made by Adamenko et al. [23], Alkindi et al. [39], koohyar et al. [42], Egorov and Makarov [20,24] were not selected for the fitting with GMA EoS but in spite of this the deviations are usually in the range ±0.1% thus reinforcing the good correlation of data with Eq. (2). Adamenko et al. [23] reported density from 290 K to 356 K but the purity of sample and the uncertainty are not given. Egorov and Makarov [24] made measurements (in 2012) between 293 K and 348 K with a pure glycerol sample but the data given by Egorov et al. [2] (in 2013) cover the range 278–348 K and thus was selected. The density measured by Darbari et al. [36], and by Xu et al. [37] are lower than the values reported by the majority of selected authors and were not selected. Also the data measured by Koohyar et al. [42] corresponding to low purity sample were not included in the fitting with GMA EoS despite the deviations of data from calculated density from Eq. (2) are below 0.1%. In Fig. 5 the density calculated from reference equation $\rho(T, p_{ref}$ = 0.1 MPa) presented by Cibulka et al. [17] was compared with GMA EoS. The relative deviations are in the range ±0.4%.

The ability of the GMA and the Tait EoS given by Cibulka et al. [17] to predict density data presented by Walsh and Rice [21] and by Dick [22] covering together the range 0.86–56.1 GPa was studied and the main results were summarized in Fig. 6. The deviations of values predicted with GMA EoS are in the range ±2% (30–50 kg·m^{-3}) much lower than those observed for Tait EoS presented by Cibulka et al. [17] for which predictions can reach 11–14% (241–390 kg·m^{-3}) at the higher pressures. In Fig. 6 the deviations between the density calculated from GMA EoS and the values reported by Egorov and Makarov [20] are also displayed. With the exception of the isotherm at 278.15 K, all the deviations are in the range 0.15% (less than 2 kg·m^{-3} at pressures close to 100 MPa).

Some mention must be made of the PVT results reported by Bridgman [1] and by McDuffie et al. [15] because of the large range

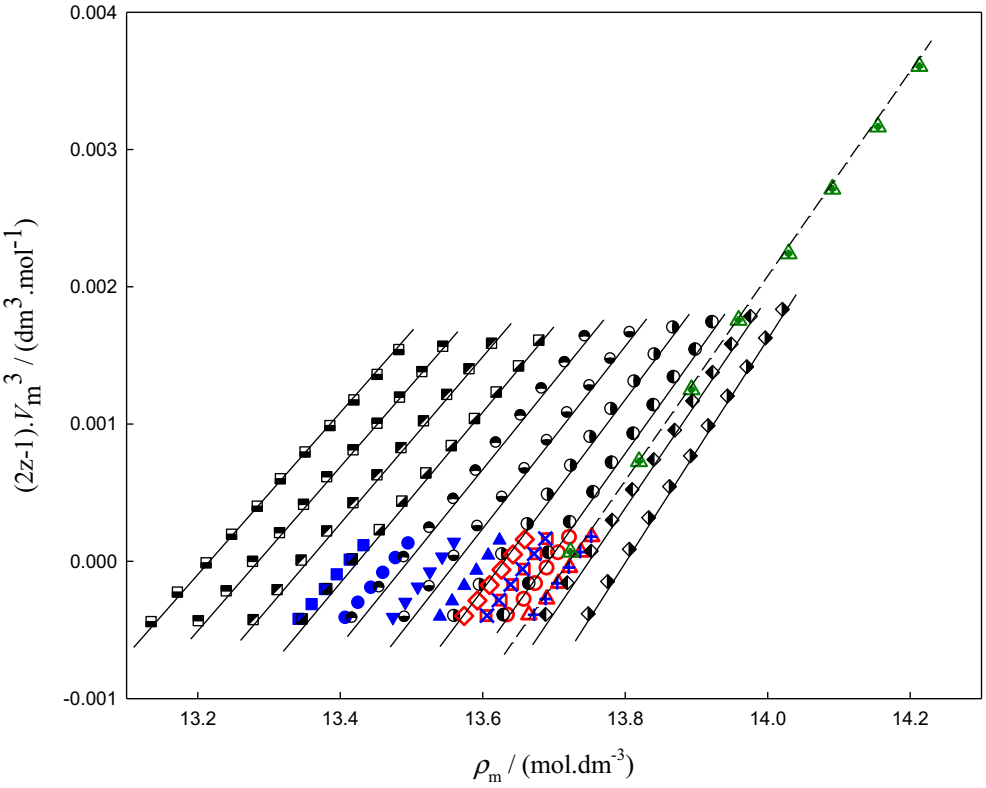

Fig. 2. Isotherms of $(2z-1)V_m^3$ versus molar density, ρ_m, for glycerol. Legend: This work purified (p) and non-purified (np) glycerol: △, 298.15 K (p); +, 298.15 (np); ○, 303.15 K (p); □, 308.15 K (p); ×, 308.15 (np); ◊, 313.15 K (p); ▲, 318.15 (np); ▼, 328.15 K (np); ●, 338.15 K (np); ■, 348.15 K (np); ⟑, 298.15 K [19]; ⟐, 283.15 [16]; ⟐, 293.15 K [16]; ◐, 303.15 K [16]; ◑, 313.15 K [16]; ◒, 323.15 K [16]; ◓, 333.15 K [16]; ◪, 343.15 K [16]; ◩, 353.15 K [16]; ⬒, 363.15 K [16]; ⬓ 373.15 K [16]. Lines calculated from GMA EoS: (—); (- - -), at T = 298.15 K.

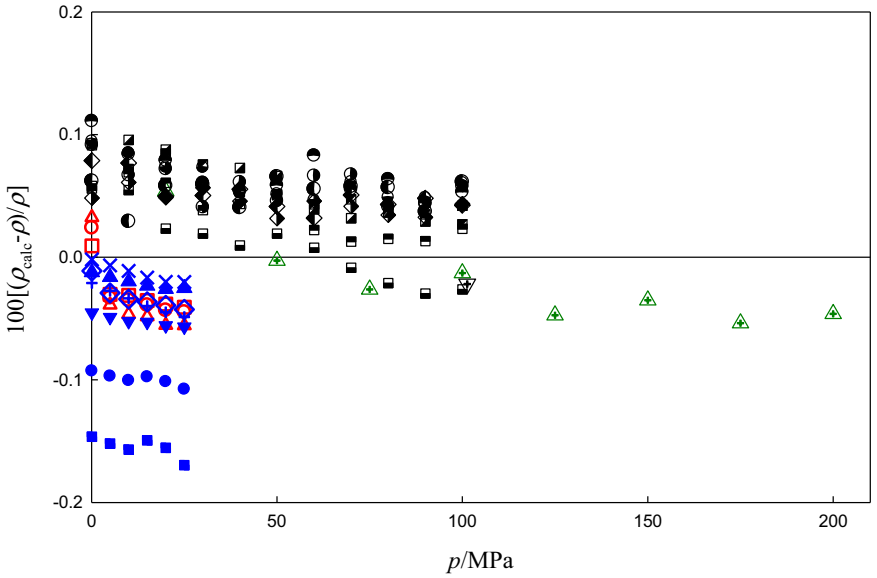

Fig. 3. Relative density deviations of glycerol between the calculated values with GMA EoS (ρ_{calc}) and the experimental values (ρ). Legend: This work purified (p) and non-purified (np) glycerol: △, 298.15 K (p); +, 298.15 (np); ○, 303.15 K (p); □, 308.15 K (p); ×, 308.15 (np); ◊, 313.15 K (p); ▲, 318.15 (np); ▼, 328.15 K (np); ●, 338.15 K (np); ■, 348.15 K (np); ⩛, 298.15 [18]; ⟑, 298.15 K [19]; ⟐, 283.15 [16]; ⟐, 293.15 K [16]; ◐, 303.15 K [16]; ◑, 313.15 K [16]; ◒, 323.15 K [16]; ◓, 333.15 K [16]; ◪, 343.15 K [16]; ◩, 353.15 K [16]; ⬒ , 363.15 K [16]; ⬓, 373.15 K [16].

of temperature and pressure involved in the measurements. The densities measured by Bridgman are too low compared with the more reliable and recent data. For example at 297.8 K and atmospheric pressure the value of 1222.6 kg·m^{-3} is reported [1]. However, from Eq. (5) the value of 1259 kg·m^{-3} is obtained. Considering all the data reported by Bridgman, positive deviations between 1.3% and 3.1% are observed. The densities calculated from the Tait EoS reported by McDuffie et al. [15] for the very accurate representation of their data were compared with the values calculated from GMA EoS in Fig. 7 for the ranges T = (283.15–343.15) K

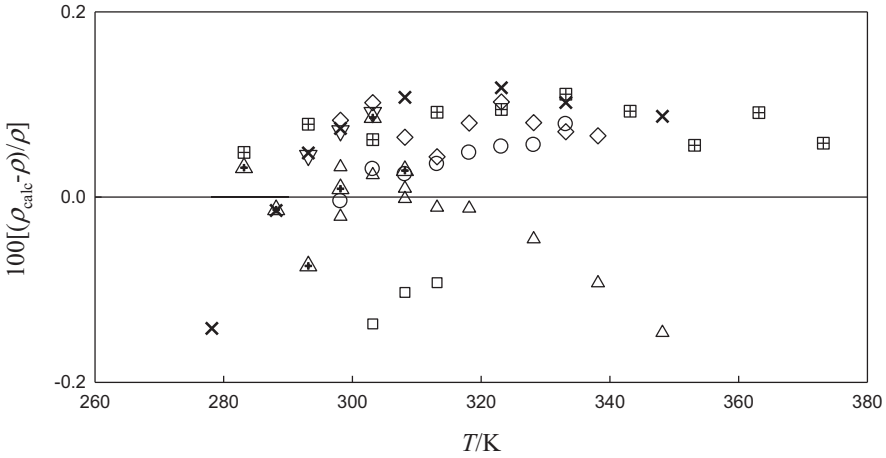

Fig. 4. Relative deviations of density as a function of temperature at atmospheric pressure for the data considered in the fitting with GMA EoS. In the calculations, ρ_{calc} is the density from GMA EoS and ρ is the corresponding experimental value. Δ, this work; ×, Egorov et al. [2]; ⊞, Khelladi et al. [16]; ○, Li et al. [38]; ⧋, Romero et al. [40]; ◇, Ge et al. [25]; □, Palani and Srinivasan [26]; ▽, Kijevcanin et al. [41].

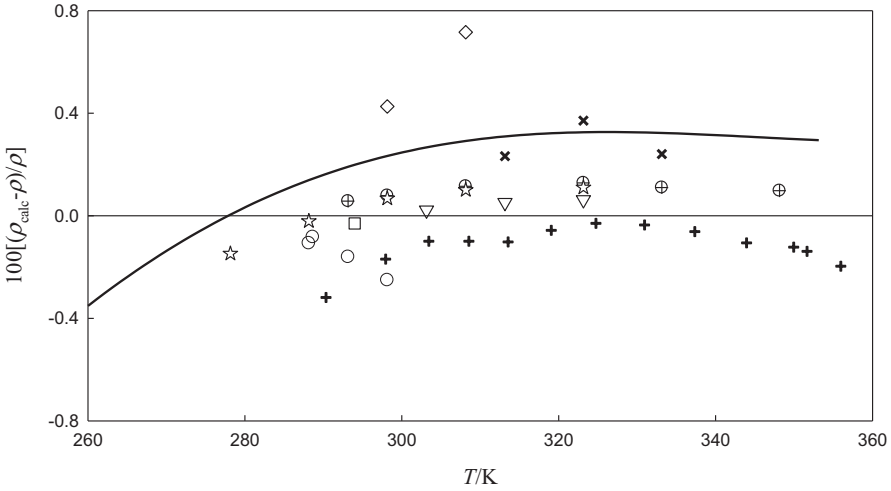

Fig. 5. Relative deviations of density as a function of temperature at atmospheric pressure for excluded data for the fitting with GMA equation. In the calculations, ρ_{calc} is the density from GMA EoS and ρ is the corresponding experimental value. ○, Bosart and Snoody [35]; ×, Darbari et al. [36]; ◇, Xu et al. [37]; +, Adamenko et al. [23]; □, Alkindi et al. [39]; ⊕, Egorov and Makarov [24]; ☆, Egorov and Makarov [20]; ▽, Koohyar et al. [42]. Solid line represents the deviation of density calculated with GMA EoS from the Tait EoS expressed by Cibulka et al. [17].

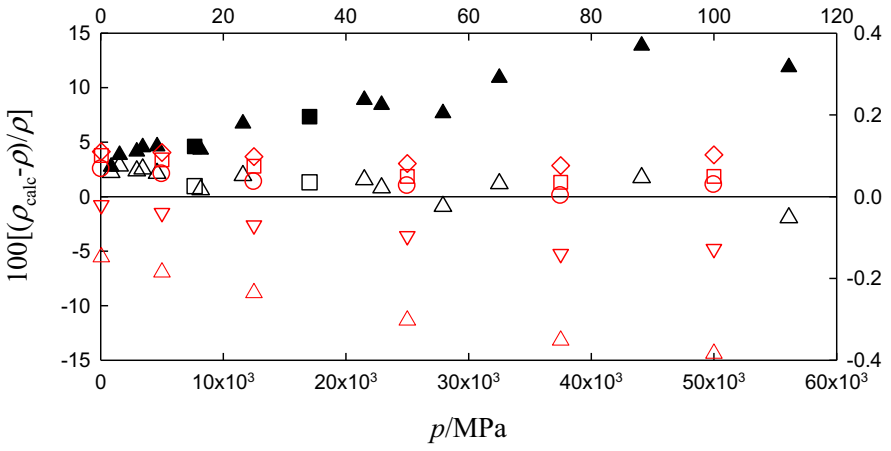

Fig. 6. Relative deviations of density between the calculated values with the GMA EoS or the Tait EoS by Cibulka et al. [17] and experimental data at very high pressure. In the calculations, ρ_{calc} is the density from GMA or Tait EoS and ρ is the experimental value. Δ, GMA EoS versus data by Dick [22]; ▲, Tait EoS versus data by Dick [22]; □, GMA EoS versus data by Walsh and Rice [21]; ■, Tait EoS versus data by Walsh and Rice [21]. The red symbols refer to comparison of GMA EoS with data from Egorov and Makarov [20] being the pressure and deviation axis given at upper and right sides, respectively: △, 278.15 K; ▽, 288.15 K; ○, 298.15 K; □, 308.15 K; ◊, 323.15 K.

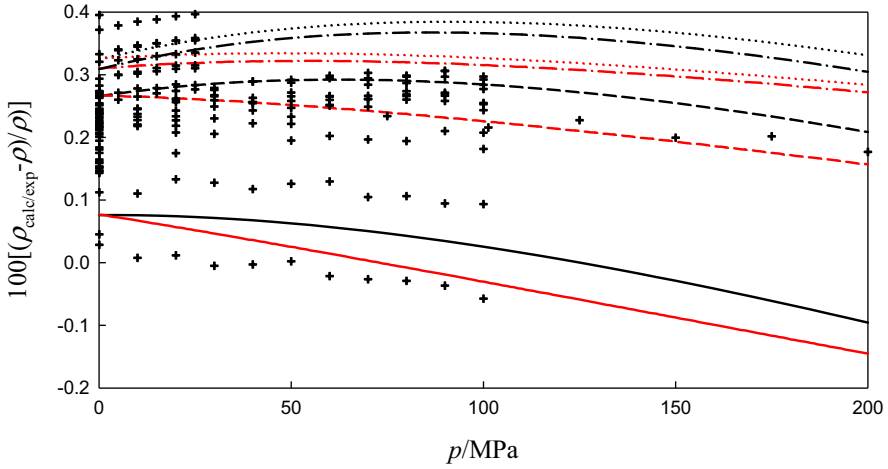

Fig. 7. Relative deviations between the calculated density with GMA EoS (ρ_{calc}) and the data from Tait EoS proposed by McDuffie et al. [15], (ρ): (—), T = 283.15 K; (- - -), T = 303.15 K; (····), T = 323.15 K; (-·-·-), T = 343.15 K. Relative deviations between the calculated density with GMA EoS (ρ_{calc}) and the data from Tait EoS by Cibulka et al. [17], (ρ): (——), T = 283.15 K; (– – –), T = 303.15 K; (····), T = 323.15 K; (—·—·—), T = 343.15 K. The crosses represent the relative deviations between the experimental densities used in the fitting with GMA EoS and the densities calculated with Tait EoS reported by Cibulka et al. [17].

and p = (0.1–200) MPa. The relative deviations are usually positive and between zero and 0.4% corresponding to maximum density deviations of about 5 kg·m^{-3}.

The most recent compilation of *PVT* data of molecular liquids including glycerol was made by Cibulka et al. [17]. They fitted the Tait EoS to experimental values from Bridgman [1], McDuffie et al. [15], Nakagawa et al. [18] and Miyamoto et al. [19]. From the fit, the standard deviation σ_ρ = 0.8 kg·m^{-3} and absolute deviation *AAD* = 0.06% result (close to the results of this work with fitting the GMA EoS). In Fig. 7 we have plotted also the relative density deviations between the data calculated from the Tait EoS reported by Cibulka et al. and from GMA EoS. The agreement between calculated densities with these models is slightly better than for the situation corresponding to Tait EoS from Mc Duffie et al. versus GMA EoS. Anyway, relative deviations are positive and also lie between zero and 0.4%. As the GMA EoS represents more recent experimental *PVT* data within ±0.05%, it can be concluded that both versions of Tait EoS must give lower densities to a maximum of 0.4% (about 5 kg·m^{-3}) compared to the experimental values. This can be concluded from Fig. 7 where the relative density deviations between the experimental data used to fit GMA EoS and the values calculated from the Tait EoS by Cibulka et al. are presented.

3.3. Mechanical coefficients

The mechanical coefficients thermal expansivity, $\alpha_p = -(1/\rho)(\partial\rho/\partial T)_p$, isothermal compressibility, $k_T = (1/\rho)(\partial\rho/\partial p)_T$, and internal pressure $p_i = (\partial U/\partial V)_T$, where U is the internal energy, were calculated from GMA EoS. The following equations are obtained [50]:

$$\alpha_p = \frac{(2B_1 + 2B_2T)\rho_m^5 + (2A_1 + 2A_2T)\rho_m^4 + 2p}{5\rho_m^5(RT^2B_0 - 2B_1T + 2B_2T^2\ln T) + 4\rho_m^4(RT^2A_0 - 2A_1T + 2A_2T^2\ln T) + RT^2\rho_m} \quad (6)$$

$$k_T = \frac{2}{\rho_m RT + 5\rho_m^5(RTB_0 - 2B_1 + 2B_2T\ln T) + 4\rho_m^4(RTA_0 - 2A_1 + 2A_2T\ln T)} \quad (7)$$

$$p_i = (B_1 + B_2T)\rho_m^5 + (A_1 + A_2T)\rho_m^4 \quad (8)$$

The internal pressure p_i can be calculated also according to the relationship

$$p_i = (\partial U/\partial V)_T = T(\partial p/\partial T)_V - p = T\cdot\gamma_V - p \quad (9)$$

where γ_V is the thermal pressure coefficient ($\gamma_V = \alpha_P/k_T$).

The density variations along isothermal or isobaric paths are usually smooth functions of temperature and pressure. However, the mechanical coefficients are quite sensitive to subtle changes in the density. The pressure behaviour of α_p isotherms, $(\alpha_p, p)_T$, has been a matter of interest due to the characteristic crossings observed for this property at high pressure and reflecting a change in the effective intermolecular potential with pressure [51]. Fig. 8 shows the behaviour of $(\alpha_p, p)_T$. The expected behaviour is observed, *i.e.* α_p decreases with the increase of pressure at isothermal conditions and it increases with the rising of the temperature at fixed pressures. The isotherms approach one another as temperature increases and close intercept at temperatures near 343 K where α_p starts to be almost independent of temperature and pressure. The minimum and maximum α_p found for the ranges of temperature and pressure studied are 2.330×10^{-4} K^{-1} for (283.15 K, 200 MPa) and 5.50×10^{-4} K^{-1} at (363.15 K, 0.1 MPa) respectively. At 298.15 K and 0.1 MPa, $\alpha_p = 4.46 \times 10^{-4}$ K^{-1}.

The isothermal compressibility is represented in the diagram $(k_T, p)_T$ of Fig. 9. The behaviour is the expected: k_T increases with temperature at isobaric conditions and decreases with pressure for fixed temperatures. The minimum and maximum values are 0.156 GPa^{-1} (at 283.15 K, 200 MPa) and 0.279 GPa^{-1} (at 363.15 K, 0.1 MPa) respectively. At 298.15 K and 0.1 MPa, k_T = 0.229 GPa^{-1}. There will be a weak influence of temperature and pressure on the compressibility of liquid glycerol compared to C_3 carbon chain alcohols – propanols and propanediols especially propanol – as evidenced by Fig. 10 where the temperature dependence of the isothermal compressibility for glycerol [17], 1-propanol [52], 2-propanol [17], 1,2-propanediol and 1,3-propanediol [17] is presented at p = 0.1 MPa. For glycerol the values calculated from GMA EoS and those from the literature are also displayed and they are in good agreement (differences between 0% and 8%). From Fig. 10 we conclude that successive inclusion of –OH groups in the carbon chain results in about a decrease by about one half in k_T. Also as more groups are added less significant will be the increase of compressibility with temperature. These differences are related with the marked differences in the H-bonded structures of the three systems. The 1-propanol has one hydroxyl group per molecule and is characterized by H-bond patterns which may be regarded as linear winding chains. Propanediols and glycerol have two and three –OH groups, per molecule, respectively and they show three-dimensional H-bonding structures which are not well

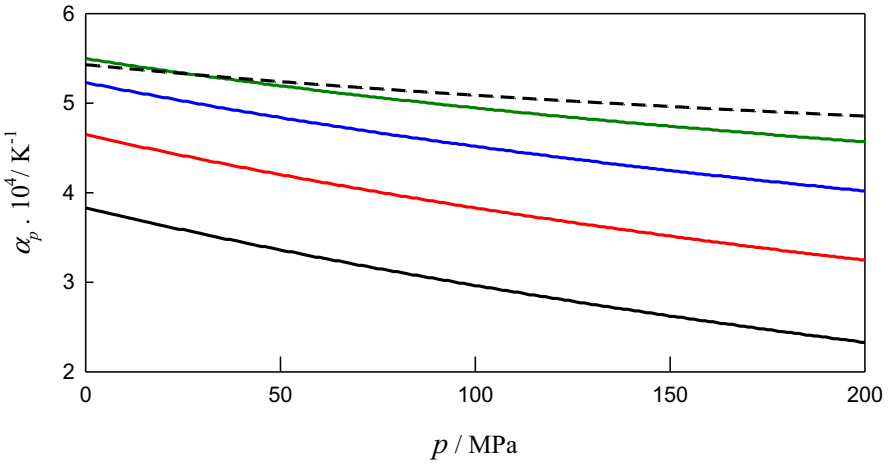

Fig. 8. Thermal expansivity, α_p, of glycerol as a function of pressure and temperature calculated from GMA EoS: (—), 283.15 K; (——) 303.15 K; (——), 323.15 K; (——), 343.15 K; (- - -), 363.15 K.

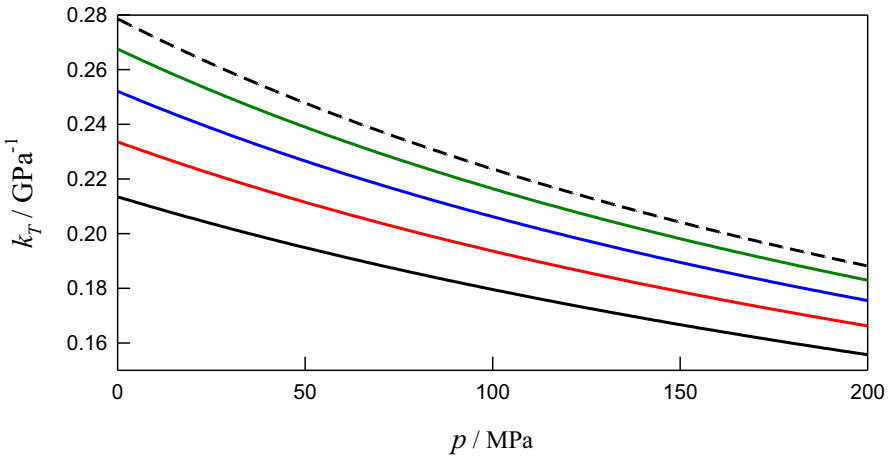

Fig. 9. Isotheral compressibility, k_T, of glycerol as a function of pressure and temperature calculated from GMA EoS: (—), 283.15 K; (——) 303.15 K; (——), 323.15 K; (——), 343.15 K; (- - -), 363.15 K.

known. The pressure dependence of k_T at 298.15 K calculated with Eq. (7) can be compared to the values obtained from compression data given by Miyamoto et al. [19]: the minimum and maximum relative deviations are 1.5% and 3.2% for 200 MPa and 0.1 MPa, respectively.

The internal pressure p_i provides a useful basis for understanding the nature of molecular interactions in the liquid state. This property is used in the study of the cohesion of liquids, reflects the molecular ordering, and provides a measure of the change in the internal energy as the liquid experiences slight isothermal expansion. The internal pressure of liquid glycerol is represented in the $(p_i, p)_T$ diagram of Fig. 11. The internal pressure is almost insensitive to the variation of pressure at temperatures higher than 343.15 K but at lower temperatures there is a significant decrease in internal pressure with rising external pressure. The temperature and pressure dependences of the internal pressure of glycerol have some resemblance to those observed for the propanediols [53]. The minimum and maximum values of internal pressure in the range (283.15–363) K and pressures up to 200 MPa are 222 MPa (at 283.15 K, 200 MPa) and 734 MPa (at 363.15 K, 200 MPa), respectively. From Fig. 11 at atmospheric pressure p_i values run between 500 MPa to 700 MPa in the range 283.15–363.15 K. At 298.15 K and atmospheric pressure p_i = 580 MPa which is close the value (p_i = 614 MPa) calculated by Zorębski [54]. Kartsev et al. [55,56] refer that at atmospheric pressure the temperature coefficient of internal pressure is sensitive to the structural organization of the liquid and reflects the character of the interactions. The liquids are classified as non- hydrogen-bonded when the temperature coefficient of p_i is negative and as hydrogen-bonded with spatial net of H-bonds when temperature coefficient of p_i is positive. From Fig. 11 the internal pressure increases with temperature and the increase is more significant at high pressure. This is possibly related with the complex three-dimensional H-bonding network of glycerol. The three –OH groups in the molecule are involved either in intramolecular and intermolecular H-bonding and the number of intermolecular bonds increases with pressure [57].

3.4. Vapour pressure and enthalpy of vapourisation

Since glycerol is an important substance in the chemical industry, it is desirable to obtain a vapour pressure equation to provide reliable vapour pressures at temperatures between the triple point and the normal boiling point. To develop an improved vapour pressure equation for glycerol a careful selection of experimental data of this property was made. In Table 3, the values from the literature for the vapour pressure of glycerol are presented. Those by Stedman [31] were obtained from the vapour pressure over (glycerol + water) mixtures of different glycerol concentration with

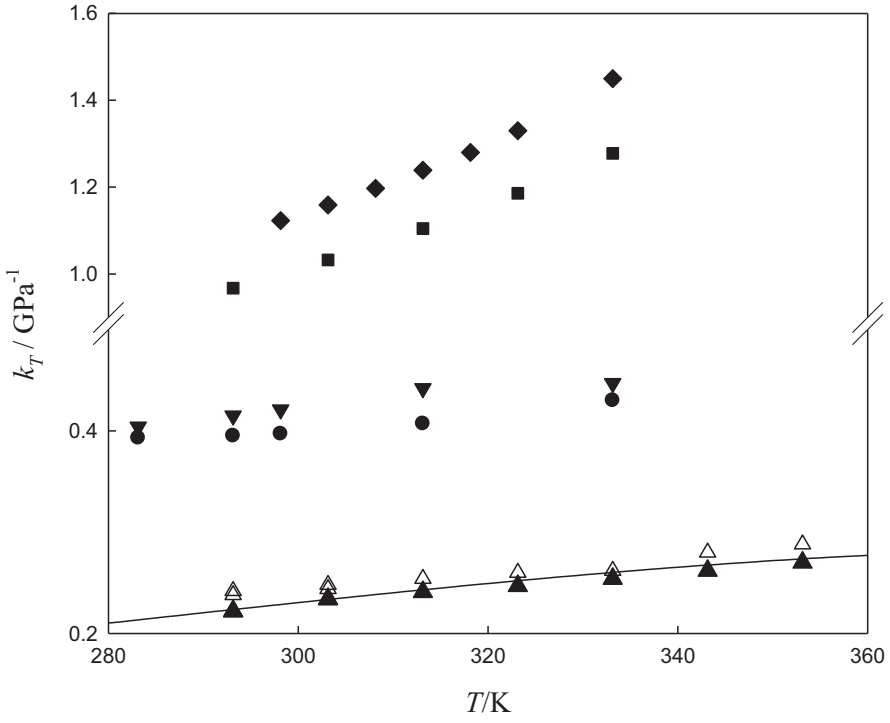

Fig. 10. Temperature dependence of isothermal compressibilities at 0.1 MPa of C_3 alcohols: ■, 1-propanol [53]; ◆, 2-propanol [17]; ▼, 1,2-propanediol [17]; ●, 1,3-propanediol [17]; ▲, glycerol [17]; Δ, glycerol (from literature) [17]; (—), glycerol from GMA EoS.

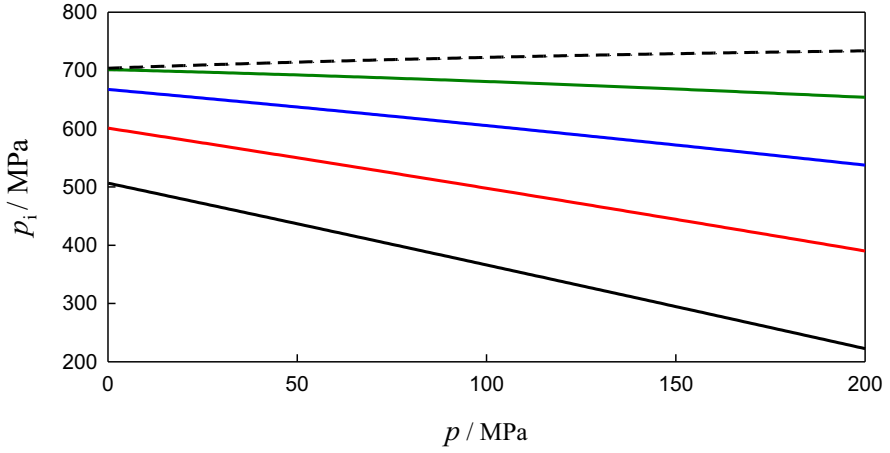

Fig. 11. Internal pressure, p_i, of glycerol as a function of pressure and temperature calculated from GMA EoS: (—), 283.15 K; (——) 303.15 K; (——), 323.15 K; (——), 343.15 K; (- - -), 363.15 K.

extrapolation to zero water content. The inclusion of these data in this work is due to the extensive temperature range of the measurements, their relative low uncertainty and the high purity of used glycerol. At the micron range, data obtained with effusion techniques by Ross and Heideger [28], and by Cammenga et al. [29] were used. However, the effusion measurements made by Zíĺberman-Granovskaya [27] in this range are too low possibly due to the thermal decomposition from repeated distillations, and were not selected. The measurements given by Filosofo et al. [46] made with a fibre manometer and those by Tang and Munkelwitz obtained from droplet evaporation [47] are also too low and they were also excluded. The values from Tatavarti et al. [48] obtained from thermogravimetric analysis are too high and were not selected. With the exception of the data by Stedman, the vapour pressures used in the medium pressure range (from 1 to 100 kPa) were measured recently [32–34]. In this range, the data from Mayer-Bugstrom [45] were not used because most of values are too low. The measurements made by Richardson [30] in extended temperature and pressure ranges are old and very low when compared with values from the selected authors. The selected values include 94 vapour pressure values covering the ranges (291.13–561.25) K and (9.293×10^{-3} to 9×10^{-3}–95.392×10^{3})

Pa of temperature and vapour pressure, respectively. These were used in a fitting procedure to obtain the parameters of the Wagner vapour pressure equation.

The Wagner equation was developed by an elaborate statistical method [5] and is written as

$$\ln\left(\frac{p^{\sigma}}{p_c}\right) = \left(\frac{T_c}{T}\right)\left(a_1 + a_2\tau^{1.5} + a_3\tau^3 + a_4\tau^6\right) \quad (10)$$

where $\tau = 1 - T_r$ with reduced temperature $T_r = T/T_c$, and the a_i are numeric adjustable parameters determined from experimental values. It has been shown that the Wagner equation represents the experimental values with high accuracy for almost all kinds of substances over the entire range from triple point to the critical point. Since enough vapour pressure data are available over a sufficiently large range of temperature, p_c can be treated as an additional adjustable parameter with reliable results [58–60]. However, attempts to obtain the critical pressure proved fruitless because the available vapour pressure values cover the region up to the normal boiling point which is too far from the critical point. With the critical coordinates measured by Nikitin et al. [4], the parameters a_i, the standard deviation of fit, and the average absolute deviations of the vapour pressure Eq. (10) are: $a_1 = -9.8298 \pm 2.0539$, $a_2 = 4.7566 \pm 4.2700$, $a_3 = -12.2243 \pm 4.3392$, and $a_4 = 4.7496 \pm 3.9189$ with corresponding correlation coefficient $r = 0.9999$. The average absolute deviation, *AAD*, and the standard deviation in vapour pressure, σ_p, were calculated using the following Eqs. (11) and (12):

$$AAD\% = 100\sum_{i=1}^{Np}|1 - p^{\sigma}_{calc}/p^{\sigma}_{exp}|_i/N_p \quad (11)$$

$$\sigma_p = \left[\sum_{i=1}^{N_p}(p_{cal} - p_{exp})_i^2/(N_p - k)\right]^{1/2} \quad (12)$$

where $p^{\sigma}{}_{cal}$ and $p^{\sigma}{}_{exp}$ are the vapour pressures calculated from Wagner equation and the experimental vapour pressure of the data point i, respectively, N_p is the number of points, and k the number of adjusted parameters ($k = 4$). The values $\sigma_p = 71$ Pa and $AAD = 6.3\%$ were obtained. The Wagner equation reproduces closely the experimental vapour pressure measurement made by McEwen very near the normal boiling point (deviation of 1.9%) and predicts $T_b = 562.90$ K, in close agreement to the value of Reid et al. [14]. In Fig. 12 the vapour pressures from the authors selected for fitting the Wagner equation are plotted and in the same figure the curve obtained from the Wagner equation is also represented between the triple point and the normal boiling point. The relative deviations of the vapour pressure calculated with Wagner equation from the experimental results is represented in Fig. 13. In this figure the selected and excluded data sets are displayed. It is observed that in the low pressure range, the values of Stedman [31] and of Camenga et al. [29] are in reasonable agreement with the calculations from the Wagner equation: the average absolute deviations are of ±5% and ±4%, respectively. In the medium range of pressure, the Kailan values are usually lower than those calculated by the Wagner equation presenting an *AAD* of ±7%. The values obtained from the Wagner equation are in very good agreement with those from Yan and Suppes [49] and Soujanya et al. [32] with *AAD* of ±1.5% and ±1.0%, respectively. The measurements by Mokbel et al. [33] show relative deviations ranging from −16.4% at the lower temperature (362 K) up to zero at 412 K. Among the 94 vapour pressure data points selected,

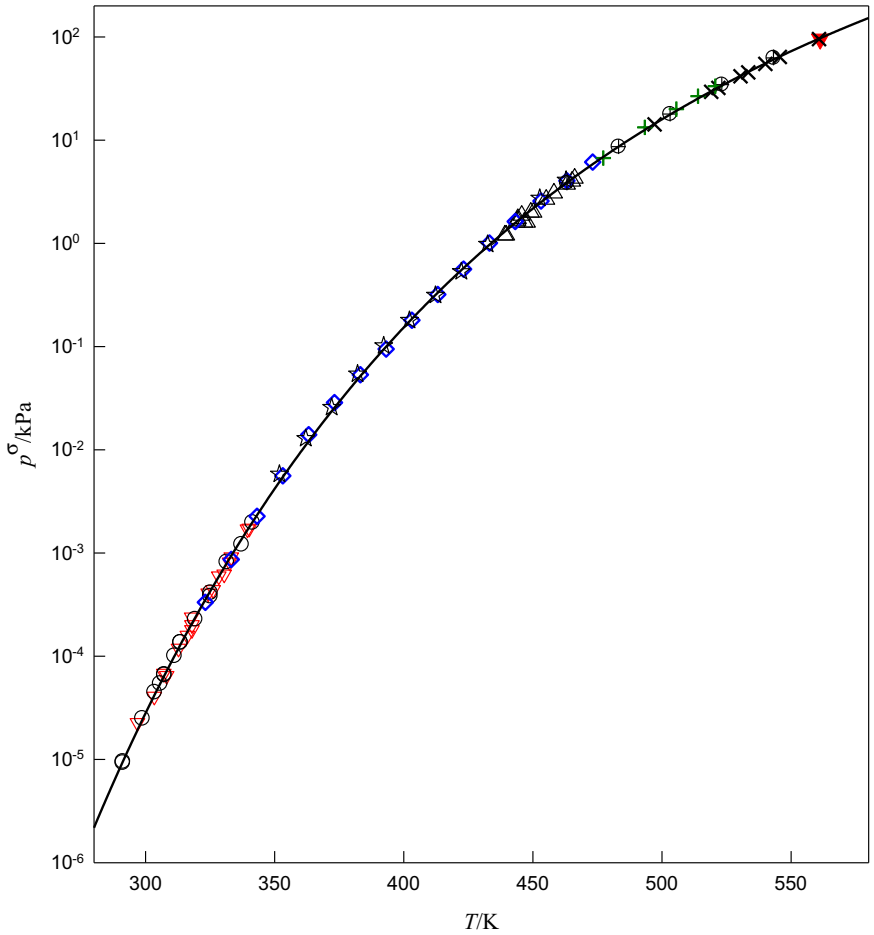

Fig. 12. Vapour pressure of glycerol. Selected experimental data: ▽, Ross and Heideger [28]; ○, Camenga et al. [29]; ◊, Stedman [31]; ×, Soujanya et al. [32]; ☆, Mokbel et al. [33]; +, Veneral et al. [34]. Δ, Kailan [43]; ⊕, Yan and Suppes [49]; ▼, McEwen [44]; (−), Eq. (10).

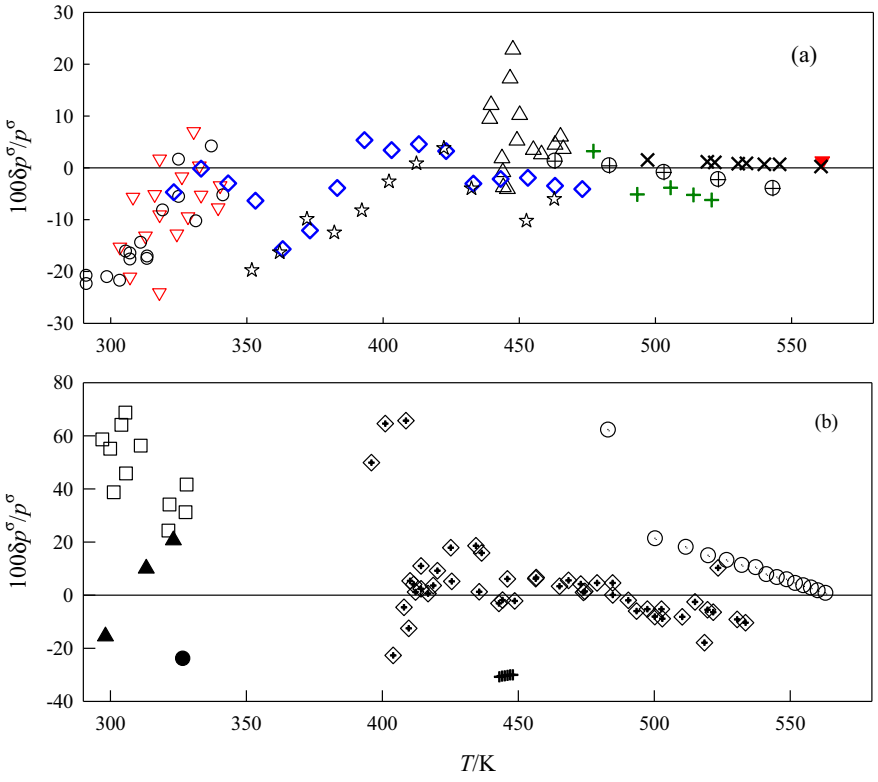

Fig. 13. Relative vapour pressure deviations calculated with the vapour pressure Eq. (10) from the experimental values as a function of temperature. For symbols, the quantity $100(\delta p^{\sigma}/p^{\sigma})$ means $100[(p^{\sigma}_{calc} - p^{\sigma})/p^{\sigma}]$, where p^{σ}_{calc} is the calculated value from Wagner equation and p^{σ} is the experimental value. (a) Selected data used in the fittings: ▽, Ross and Heideger [28]; ○, Camenga et al. [29]; ◊, Stedman [31]; ×, Soujanya et al. [32]; ☆, Mokbel et al. [33]; +, Veneral et al. [34]. Δ, Kailan [43]; ⊕, Yan and Suppes [49]; ▼, McEwen [44]. (b) Data rejected for the fitting: ◈, Richardson [30]; ●, Zilberman-Granovskaya [27]; ◯, Mayer-Bugstrom [45]; ▲, Filosofo et al. [46]; □, Tang and Munkelwitz [47]; +, Tatavarti et al. [48].

65% have relative deviations in the range ±5% a value which is lower than the experimental error in the micron range and close to the uncertainty of measurements in the low temperature range (vapour pressures 0.1–500 Pa). Therefore the Wagner equation provides a good overall performance in the calculation of the vapour pressure between the triple point and normal boiling point. Because of the data discrepancy observed within the micron and low pressure ranges, it will be advisable to perform new measurements of vapour pressure with high purity samples.

For most of pure substances, the experimental information for the enthalpy of vapourisation exists only at the normal boiling point. For glycerol, calorimetric determinations of the enthalpy of vapourisation are missing and the existing calculated data refer to room temperature, well below the normal boiling point. The only calorimetric value of the enthalpy of vapourisation was reported at 298.15 K by Bastos et al. [61]: $\Delta^g_l H_m\,(T = 298.15\ K) = (91.7 \pm 0.9)\ \mathrm{kJ{\cdot}mol^{-1}}$.

In the temperature range between the triple point and normal boiling point, the vapour pressure is low and thus perfect gas behaviour can be assumed for the gaseous phase at liquid vapour coexistence. Also in this range the molar volume of the liquid is negligible compared with that of vapour phase. With this assumptions, the calculation of the enthalpy of vapourisation at any generic temperature, $\Delta^g_l H_{\mathrm{m}}\,(T)$, can be made from the knowledge of this property at a temperature T_{i}, $\Delta^g_l H_{\mathrm{m}}\,(T_{\mathrm{i}})$ using the relationship:

$$\Delta^g_l H_{\mathrm{m}}(T) \cong \Delta^g_l H_{\mathrm{m}}(T_i) + \int_{Ti}^{T} \Delta^g_{\ell} C_{p,m}\,(T)dT \qquad (13)$$

where $\Delta^g_l C_{p,\mathrm{m}} = C^{pg}_{p,m} - C^{l}_{p,m}$, is the change in molar heat capacity on vapourisation: $C^{pg}_{p,m}$ is the perfect gas molar heat capacity and $C^{l}_{p,m}$ the molar liquid heat capacity. The perfect gas heat capacity is well represented by the polynomial equation [14]:

$$C^{pg}_{p,m}(T)/(\mathrm{J\cdot K^{-1}\cdot mol^{-1}}) = 8.424 + 0.4442\,(T/\mathrm{K}) - 3.159 \cdot 10^{-4}\,(T/\mathrm{K})^2 + 9.378 \cdot 10^{-8}(T/\mathrm{K})^3 \qquad (14)$$

Eq. (14) follows very closely the simulation results obtained by Borghi et al. [62]. For the heat capacity of the liquid, the experimental values of Gibson and Giauque [63] in the range (193–299) K, of Righetti et al. [64] at (298–383) K, and of Gateev [65] for (293–513) K are in good agreement. Thus they are combined to fit the equation:

$$C^{l}_{p,m}(T)/(\mathrm{J\cdot K^{-1}\cdot mol^{-1}}) = 112.6 + 0.2635\,(T/\mathrm{K}) + 3.143 \cdot 10^{-4}\,(T/\mathrm{K})^2 \qquad (15)$$

with standard deviation $\sigma = \pm 1.8\ \mathrm{J{\cdot}K^{-1}\ mol^{-1}}$. Using the reference $\Delta^g_l H_m\,(T_i = 298.15\ \mathrm{K})$ by Bastos et al. [61] and the Eqs. (14) and (15), the enthalpy of vapourisation was calculated between the triple point and the normal boiling point from Eq. (13). The results are plotted in Fig. 14.

At every first order phase transition, the (liquid + vapour) equilibrium is governed by the Clapeyron equation:

$$dp^{\sigma}/dT = \Delta^g_{\ell} H_m/(T \cdot \Delta^g_{\ell} V_m) \qquad (16)$$

The simplifying assumptions made before for the vapour and liquid phases applied to the Clapeyron equation lead to:

$$\Delta^g_{\ell} H_m = RT^2\,(d\,\mathrm{ln}p^{\sigma}/dT) \qquad (17)$$

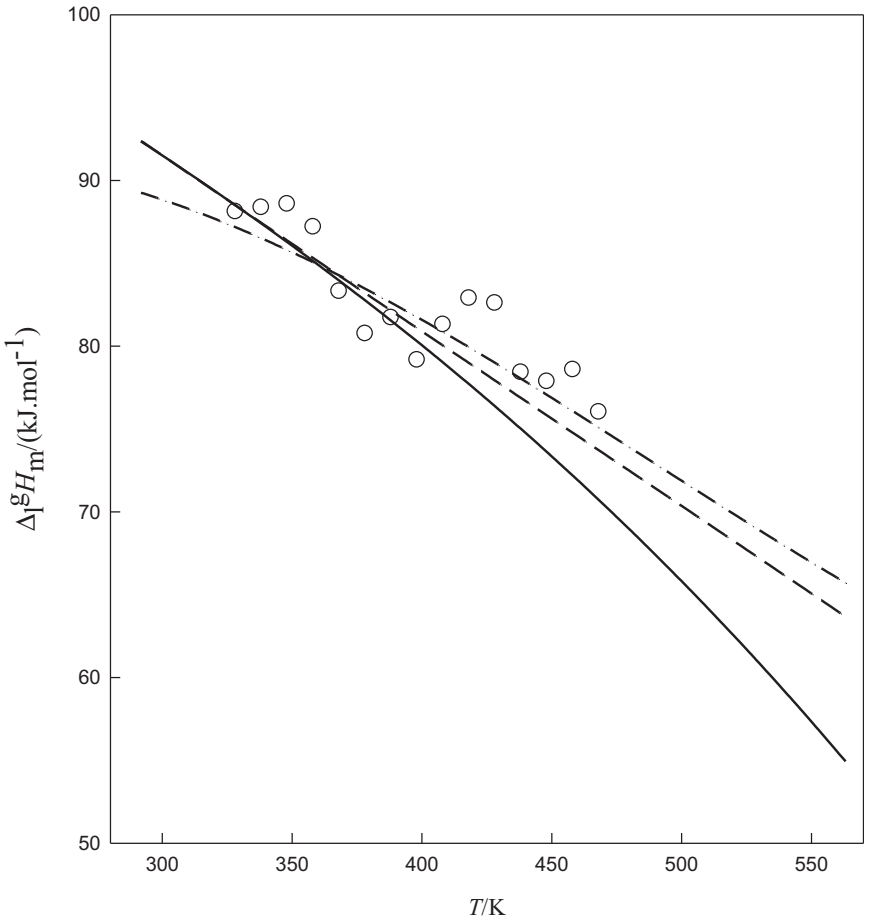

Fig. 14. Molar enthalpy of vapourisation of glycerol. (○), Stedman [31], (▬) Eqs. (13)–(15); (- - -), Eqs. (13), (14) and (19); (-·-·-), Eq. (17).

Eqs. (13) and (17) constitute independent methods for the calculation of enthalpy of vapourisation as a function of the temperature. The values of enthalpy of vapourisation calculated from Eq. (17) are also plotted in Fig. 14. Increasing differences in the enthalpy of vapourisation calculated from Eqs. (13) and (17) are observed with the increase of temperature: at the normal boiling point the values of enthalpy of vapourisation are 54.9 kJ·mol^{-1} and 65.7 kJ·mol^{-1}, respectively. These differences can be possibly explained by the overestimation of the change $\Delta_l^g C_{p,m}$ with the use of Eq. (15) for the calculation of molar liquid heat capacity. This equation gives $\Delta_l^g C_{p,m} = -186$ J·K^{-1}·mol^{-1} at the normal boiling point. Considering the assumptions that the gaseous phase behaves as a perfect gas and that the molar volume of the liquid is of negligible value when compared with the molar volume of the vapour, the change in the molar heat capacity can be calculated from the Wagner equation (10) as:

$$\Delta_l^g C_{p,m} = R\,T_r\left(\frac{3a_2}{4\sqrt{\tau}} + 6a_3\tau + 30a_4\tau^4\right) \qquad (18)$$

At the normal boiling point Eq. (18) gives – 92 J·K^{-1}·mol^{-1}, which is about one half the $\Delta_l^g C_{p,m}$ value calculated from Eqs. (14) and (15). Omelchenko [66] expressed the molar liquid heat capacity measured by several Russian researchers, by the following equation

$$C_{p,m}^l/(\mathrm{J\cdot K^{-1}\cdot mol^{-1}}) = 137.654 + 0.3184\,(T/\mathrm{K}) - 1.125 \cdot 10^{-4}\,(T/\mathrm{K})^2 \qquad (19)$$

Eqs. (14) and (19) give $\Delta_l^g C_{p,m} = -107.5$ J·K^{-1}·mol^{-1} at the normal boiling point, close to the value obtained from Eq. (18). Also the values of the enthalpy of vapourisation calculated from Eq. (13) with Eqs. (14) and (19) are very close to those resulting from the Clapeyron equation as seen in Fig. 14. The differences are less than 2.0 kJ·mol^{-1} and at normal boiling point the average between the values from the two equations is $\Delta_l^g H_m\,(T = T_b)$ = (64.7 ± 1.0) kJ·mol^{-1}.

The values of the enthalpy of vapourisation calculated by Stedman [31] considered as representative for glycerol [67,68] were also plotted in Fig. 14. They show some dispersion but a general good agreement is observed with the values calculated from Eqs. (13) and (17).

Using a realistic potential model to describe the large internal flexibility of the glycerol molecule, Chelli et al. [69] studied the thermodynamic properties of the liquid and glassy state of this substance. They obtained $\Delta_l^g H_m\,(T = 298.15\ \mathrm{K})$ = (73.0 ± 2.5) kJ·mol^{-1}. This value is 20% lower than the calorimetric value reported by Bastos et al. [61] and 15–17% lower than values reported in the literature: 85.8 kJ·mol^{-1} [28], (86.8 ± 0.7) kJ·mol^{-1} [29], and (88.2 ± 0.9) kJ·mol^{-1} [33]. At T = 298.15 K, Clapeyron equation gives $\Delta_l^g H_m$ = 88.9 kJ·mol^{-1} in close agreement to the calorimetric determination by Bastos et al. [61].

4. Conclusions

New density values for glycerol were measured from 298.15 K to 348.15 K and pressures up to 25.0 MPa with an estimated com-

bined standard uncertainty of 0.86 kg·m^{-3}. These data combined with selected values from the literature covering the overall ranges (278.15–373.15) K and (0.1–200) MPa were used to fit the GMA EoS. The correlation of data with this EoS is very good with resulting average absolute deviation and standard deviation of ±0.05% and ±0.8 kg·m^{-3}, respectively. One very important feature is the ability of the GMA EoS to predict the density at extremely high pressures (up to 60 GPa) with reasonable accuracy.

The mechanical coefficients were calculated from the GMA EoS and the main findings can be summarized as follows. The thermal expansivity increases with the temperature at isobaric conditions as expected, and for temperatures higher than 350 K this property reaches an almost constant value independent of temperature and pressure. The isothermal compressibility is low. It is about one half of the values for propanediols at $p = 0.1$ MPa. The values of this property predicted with GMA EoS are in good agreement with data from the literature. The internal pressure of glycerol is high (*ca.* 600 MPa at atmospheric pressure) and increase with temperature for isobaric conditions especially at high pressure.

The vapour pressure values for glycerol from the literature available in the range (291–561) K corresponding to the pressure range (9×10^{-3}–95.392×10^{3}) Pa were used to fit the Wagner vapour pressure equation with coordinates at the critical point determined by Nikitin et al. [4]. Relative deviations between calculated and experimental values are usually in the range ±5% in the micron range and about ±1% near the normal boiling point. Due to the experimental vapour pressure discrepancy observed at the micron and low pressure ranges, it will be important to make new measurements in these ranges.

The enthalpy of vapourisation of glycerol was calculated between the triple point and the normal boiling point following two routes: using calorimetric data and from the Clapeyron equation. The calculated enthalpy of vapourisation from both routes differs by less than 2 kJ·mol^{-1}. From the calculations using calorimetric results, we conclude that even today a consistent set of measurements of heat capacity of the liquid glycerol at temperatures above 300 K is missing.

Acknowledgments

This research is sponsored by FEDER funds through the program COMPETE – Programa Operacional Factores de Competitividade – and by national funds through FCT – Fundação para a Ciência e a Tecnologia, under the project PEst-C/EME/UI0285/2013, and was also supported by a grant, EADIC II – ERASMUS MUNDUS ACTION 2 LOT 13A UE Mobility Programme 2010-2401/001-001 – EMA2. This work was done within the framework of the project EMSURE – W.P.4 of the program Energy and Mobility for Sustainable Regions.

References

[1] P.W. Bridgman, Proc. Am. Acad. Arts Sci. 67 (1932) 1–27.
[2] G.I. Egorov, D.M. Makarov, A.M. Kolker, Therm. Acta. 570 (2013) 16–26.
[3] E.K. Goharshadi, A. Morsali, M. Abbaspour, Fluid Phase Equilib. 230 (2005) 170–175.
[4] E.D. Nikitin, P.A. Pavlov, P.V. Skripov, J. Chem. Thermodyn. 25 (1993) 869–880.
[5] W. Wagner, Cryogenics 13 (1973) 470–482.
[6] C.E. Ferreira, N.M.C. Talavera-Prieto, I.M.A. Fonseca, A.T.G. Portugal, J. Chem. Thermodyn. 47 (2012) 183–196.
[7] Private communication from Anton Paar, 2005.
[8] O. Fandiño, J. Garcia, M.P.J. Comuñas, E.R. López, J. Fernández, Ind. Eng. Chem. Res. 45 (2006) 1172–1182.
[9] P.N. Shankar, M. Kumar, Proc. R. Soc. Lond. 444 (1994) 573–581.
[10] R.L. Cook, H.E. King, C.A. Herbst, D.R. Herschbach, J. Chem. Phys. 100 (1994). 5178-518.
[11] R.C. Wilhoit, J. Chao, K.R. Hall, J. Phys. Chem. Ref. Data 14 (1985) 1–175.
[12] M. Volmer, M. Marder, Z. Physik, Chem. 154 (1931) 97–112.
[13] http://webbook.nist.gov/chemistry/fluid/.
[14] R.C. Reid, J.M. Prausnitz, B.E. Poling, The Properties of Gases and Liquids, fourth ed., McGraw-Hill, New York, 1987.
[15] G.E. McDuffie, J.W. Forbes, W.M. Madigosky, J.J. von Bretzel, J. Chem. Eng. Data 14 (1969) 176–180.
[16] H. Khelladi, F. Plantier, J.L. Daridon, H. Djelouah, Ultrasonics 49 (2009) 668–675.
[17] I. Cibulka, L. Hnedkovsky, T. Takagi, J. Chem. Eng. Data 42 (1997) 415–433.
[18] M. Nakagawa, Y. Miyamoto, T. Moriyoshi, J. Chem. Thermodyn. 15 (1983) 15–21.
[19] Y. Miyamoto, M. Takemoto, M. Hosokawa, Y. Uosaki, T. Moriyoshi, J. Chem. Thermodyn. 22 (1990) 1007–1014.
[20] G.I. Egorov, D.M. Makarov, J. Chem. Thermodyn. 79 (2014) 135–158.
[21] J.M. Walsh, M.H. Rice, J. Chem. Phys. 26 (1957) 815–823.
[22] R.D. Dick, J. Chem. Phys. 74 (1981) 4053–4061.
[23] I.I. Adamenko, L.A. Bulavin, V. Ilyin, S.A. Zelinsky, K.O. Moroz, J. Mol. Liq. 127 (1–3) (2006) 90–92.
[24] G.I. Egorov, D.M. Makarov, J. Solut. Chem. 41 (2012) 536–554.
[25] M.-L. Ge, J.-L. Ma, B. Chu, J. Chem. Eng. Data 55 (2010) 2649–2651.
[26] R. Palani, G. Srinivasan, Int. J. Eng. Res. Tech 10 (2012). ISSN: 2278-0181.
[27] A.A. Zílberman-Granovskaya, Zh. Fiz. Khim. 14 (1940) 759.
[28] G.R. Ross, W.J. Heideger, J. Chem. Eng. Data 7 (1962) 505–507.
[29] H.K. Cammenga, F.W. Schulze, W. Theuerl, J. Chem. Eng. Data 22 (1977) 131–134.
[30] A. Richardson, J. Chem. Soc. 49 (1889) 761–776.
[31] D.F. Stedman, Trans. Faraday Soc. 24 (1928) 289–298.
[32] J. Soujanya, B. Styavathi, T.E.V. Prasad, J. Chem. Thermodyn. 42 (2010) 621–624.
[33] I. Mokbel, T. Sawaya, M-Line Zanota, R.A. Naccoul, J. Jose, C. Bellefon, J. Chem. Eng. Data 57 (2012) 284–289.
[34] J.G. Veneral, T. Benazzi, M.A. Mazutti, F.A.P. Voll, L. Cardozo-Filho, M.L. Corazza, R. Guirardello, J.V. Oliveira, J. Chem. Thermodyn. 58 (2013) 398–404.
[35] L.W. Bosart, A.O. Snoody, Ind. Eng. Chem. 19 (1927) 506–510.
[36] G.S. Darbari, R.P. Singh, G.S. Verma, S. Rajagopalan, Nuovo Cimento B52 (1967) 1–17.
[37] L. Xu, X. Hu, R. Lin, J. Solut. Chem. 32 (2003) 363–370.
[38] Q.S. Li, M.G. Su, S. Wang, J. Chem. Eng. Data. 52 (2007) 1141–1145.
[39] A.S. Alkindi, Y.M. Al-Wahaibi, A.H. Muggeridge, J. Chem. Eng. Data 53 (2008) 2793–2796.
[40] C.M. Romero, M.S. Paez, D. Perez, J. Chem. Thermodyn. 40 (2008) 1645–1653.
[41] Lj.M. Kijevčanin, E.M. Živković, B.D. Djordjević, I.R. Radović, J. Jovanović, S.P. Šerbanović, J. Chem. Thermodyn. 56 (2013) 49–56.
[42] F. Koohyar, A.A. Rostami, M.J. Chaichi, F. Kiani, J. Solut. Chem. 40 (2011) 1361–1370.
[43] A. Kailan, Anal. Chem. 51 (1912) 81–101.
[44] B.C. McEwen, J. Chem Soc. 123 (1923) 2279–2285.
[45] Mayer-Bugstrom, Z.deut.Ol-Fett-Ind. 44 (1924) 417–418.
[46] I. Filosofo, M. Merlin, A. Rostagni, Nuovo Cimento 7 (1950) 69–75.
[47] I.N. Tang, H.R. Munkelwitz, J. Colloid Interface Sci. 141 (1991) 109–118.
[48] A.S. Tatavarti, D. Dollimore, K.S. Alexander, AAPS Pharma Sci. 4 (2002) 1–12.
[49] W. Yan, G.J. Suppes, Chem. Eng. Data 53 (2008) 284–289.
[50] E.K. Goharshadi, M. Moosavi, J. Mol. Liq. 142 (2008) 41–44.
[51] S.L. Randzio, Phys. Lett. A 117 (1986) 473–476.
[52] G. Watson, T. Lafitte, C.K. Zéberg-Mikkelsen, A. Baylaucq, D. Bessieres, C. Boned, Fluid Phase Equilib. 247 (2006) 121–134.
[53] E. Zorębski, M. Piotrowska, M. Dzida, Acta Phys. Pol. 114 (2008) A265–A270.
[54] E. Zorębski, Mol. Quant. Acoust. 26 (2005). 317-26.
[55] V.N. Kartsev, M.N. Rodnikova, I. Bartel, S.N. Shtykov, Russian, J. Phys. Chem. 76 (2002) 1016–1018.
[56] V.N. Kartsev, J. Struct. Chem. 45 (2004) 832–837.
[57] L.J. Root, B.J. Berne, J. Chem. Phys. 107 (1997) 4350–4357.
[58] C. Henderson, D.G. Lewis, P.C. Prichard, L.A.K. Staveley, I.M.A. Fonseca, L.Q. Lobo, J. Chem. Thermodyn. 18 (1986) 1077–1088.
[59] G. Cubitt, C. Henderson, L.A.K. Staveley, I.M.A. Fonseca, A.G.M. Ferreira, L.Q. Lobo, J. Chem. Thermodyn. 19 (1987) 703–710.
[60] H. Streatfeild, C. Henderson, L.A.K. Staveley, A.G.M. Ferreira, I.M.A. Fonseca, L. Q. Lobo, J. Chem. Thermodyn. 19 (1987) 1163–1171.
[61] M. Bastos, S.-O. Nilsson, M.D.M.C. Ribeiro da Silva, M.A.V. Ribeiro Da Silva, I. Wadso, J. Chem. Thermodyn. 20 (1988) 1353–1359.
[62] D.F. Borghi, C.R.A. Abreu, R. Guirardello, Thermochemical properties estimation for biodiesel related mixtures, in: Proceedings of the International Conference on Engineering Optimization, Rio de Janeiro, 2012.
[63] G.E. Gibson, W.F. Giauque, J. Am. Chem. Soc. 45 (1922) 93–104.
[64] M.C. Righetti, G. Salvetti, E. Tombari, Thermochim. Acta 316 (1998) 193–195.
[65] S.B. Gateev, Izvestiya VTI 10 (1950).
[66] F.S. Omelchenko, in: Izv. Vyssh. Uchebn. Zaved, Pisch. Tkhnol. 3 (1962) 97–98.
[67] http://www.dow.com/optim/optim-advantage/physical-properties/heat_vapour.htm.
[68] E. Jungermann, N.O.V. Sonntag, Glycerine: A Key Cosmetic Ingredient, CRC Press, 1991.
[69] R. Chelli, P. Procacci, G. Cardini, S. Califano, Phys. Chem. Chem. Phys. 1 (1999) 879–885.